

**Unraveling the impact of Ag dopant in Zn-In-S colloidal nanocrystals  
for boosting visible-light-driven photocatalytic CO<sub>2</sub> reduction**

Jing Wang,<sup>a</sup> Shenshen Ouyang,<sup>a</sup> Ye Wang,<sup>a</sup> Xusheng Wang,<sup>b</sup> Xiaohui Ren,<sup>c</sup> Li Shi<sup>a\*</sup>

<sup>a</sup> School of Materials Science and Chemical Engineering, Ningbo University, Ningbo, Zhejiang,  
315211, P. R. China.

<sup>b</sup> School of Materials Science and Engineering, Zhejiang Sci-Tech University, Hangzhou 310018,  
China.

<sup>c</sup> The State Key Laboratory of Refractories and Metallurgy, School of Materials and Metallurgy,  
Wuhan University of Science and Technology, Wuhan 430081, China.

E-mail: shili1@nbu.edu.cn

## **Experimental section**

### **Chemicals**

N, N-dimethylformamide (DMF, >99.9%) and aqueous ammonia solution (25%-28%) were purchased from Macklin. Silver nitrate ( $\text{AgNO}_3$ , 99.8%) were purchased from Aladdin, zinc nitrate ( $\text{Zn}(\text{NO}_3)_2$ , 99.0%) were purchased from Shanghai Pilot Enterprise, mercaptoacetic acid (MAA, 70%) were purchased from Sigma-Aldrich, sodium sulphide ( $\text{Na}_2\text{S}\cdot 9\text{H}_2\text{O}$ , 99%) and  $\text{InCl}_3$  (99.99%) were purchased from damas-beta. All experimental requirements were configured using distilled water.

### **Synthesis of Ag-ZnInS colloidal crystals**

The preparation procedures of Zn-In-S colloidal crystals are described as below. Under high speed stirring, 0.5 mL of  $\text{Zn}(\text{NO}_3)_2$  (1.0 M) and 2.0 mL of MAA (1.0 M) were added one by one into 8 mL of  $\text{H}_2\text{O}$  to form a white flocculent suspension. After adding 0.6 mL of  $\text{NH}_4\text{OH}$  (5.0 M), the solution became transparent. After that, 1 mL of 1.0 M  $\text{InCl}_3$  containing 0.2 M  $\text{HNO}_3$  were added. Subsequently, 1.0 mL of 1.0 M fresh  $\text{Na}_2\text{S}$  solution was dropped quickly. After stirring for 2 min, the above mixed solution was put into an oil bath and kept at  $90^\circ\text{C}$  for 30 min. After cooling down to room temperature, the colloidal crystals were collected by centrifugation and washed three times with 40 mL of ethanol, then dried under  $60^\circ\text{C}$  overnight. Ag doped Zn-In-S samples with different amounts of Ag were prepared using the same procedures as described above except that 0.1 ml, 0.2 ml and 0.4 ml of  $\text{AgNO}_3$  (0.1 M) was added together with  $\text{Zn}(\text{NO}_3)_2$ , and three samples 1Ag-ZnInS, 2Ag-ZnInS, and 3Ag-ZnInS were produced, respectively.

### **Photocatalytic $\text{CO}_2$ reduction**

The photoreduction of  $\text{CO}_2$  was carried out in an All Glass Automatic on-Line Trace Gas Analysis

System (Labsolar-6A, Beijing Perfectlight). A 300 W Xenon lamp (PLS-SXE300+) combined with a UV cutoff filter ( $\lambda > 420\text{nm}$ ,  $160\text{ mW cm}^{-2}$ ) was used as the visible light source. The entire reaction was carried out in a liquid-solid reaction system and a DC-0506 low temperature thermostat tank (Shanghai, bilon) was used to maintain the temperature of the reaction cell at about  $10^\circ\text{C}$ . In a typical procedure, 2,2'-bipyridine (25mg) and 0.2 ml of  $\text{CoCl}_2$  (0.01 M) were added into 35 ml of DMF in a quartz reactor under stirring. The prepared Ag-ZnInS colloidal crystal powder (20 mg) was dispersed in the above reaction solution under vigorous stirring, and continuously sonicated for 5 minute to ensure uniform dispersion of the sample in DMF, after which 7 ml of TEOA was dropped in under continuous stirring. The reactor was set in the system, which was then evacuated to ensure that no air gases ( $\text{O}_2$  and  $\text{N}_2$ ) were detected. High quality  $\text{CO}_2$  (99.999%) was then injected until the pressure reached 80 kPa. The product  $\text{CO}$  and  $\text{H}_2$  were detected automatically per hour by an on-line gas chromatograph (Agilent 8860 GC System with TCD and FID detector, American). The isotope experiment was conducted according to the same procedures as described above except that  $^{13}\text{CO}_2$  gas was used as the reactant. After reaction for 5 h, 1 ml gas was extracted by a sampling needle, which was injected into the gas chromatograph-mass spectrum machine (JEOL-GCQMS, JMS-K9 and 6890N Network GC system, Agilent) for the analysis of  $\text{CO}$  product.

### **Characterization**

The crystal structure of colloidal crystals was analyzed by powder X-ray diffraction (XRD, Bruker D8). A transmission electron microscope (JEOL JEM 2100F) was utilized to take the transmission electron microscopy (TEM), high-resolution TEM (HRTEM) and Energy Dispersive X-Ray Spectroscopy (EDS) mapping images. X-ray photoelectron spectroscopy (XPS, Thermo Scientific K-Alpha+) was used to measure the chemical states of colloidal crystals. A fluorescence

spectrophotometer F-7100PL was used to record the PL spectra of the samples, and a steady-state fluorescence spectrometer (Edinburgh FLS1000) was used to record the time-resolved decay spectra of the samples. Ultraviolet–visible spectroscopy (METASH) was used to collect the optical properties of the samples. The weight percentage of Ag was measured by inductively coupled plasma optical emission spectrometer (ICP-OES, Agilent 5110). The ultraviolet photoelectron spectroscopy (Thermo ESCALAB XI+) was used to record the band structure of samples.

Table S1. ICP-OES data of Ag-ZnInS colloidal nanocrystals with different amount of Ag dopant.

sample	Weight percentage of Ag in Zn-In-S (wt%)
1Ag-ZnInS	0.69
2Ag-ZnInS	1.13
3Ag-ZnInS	2.13

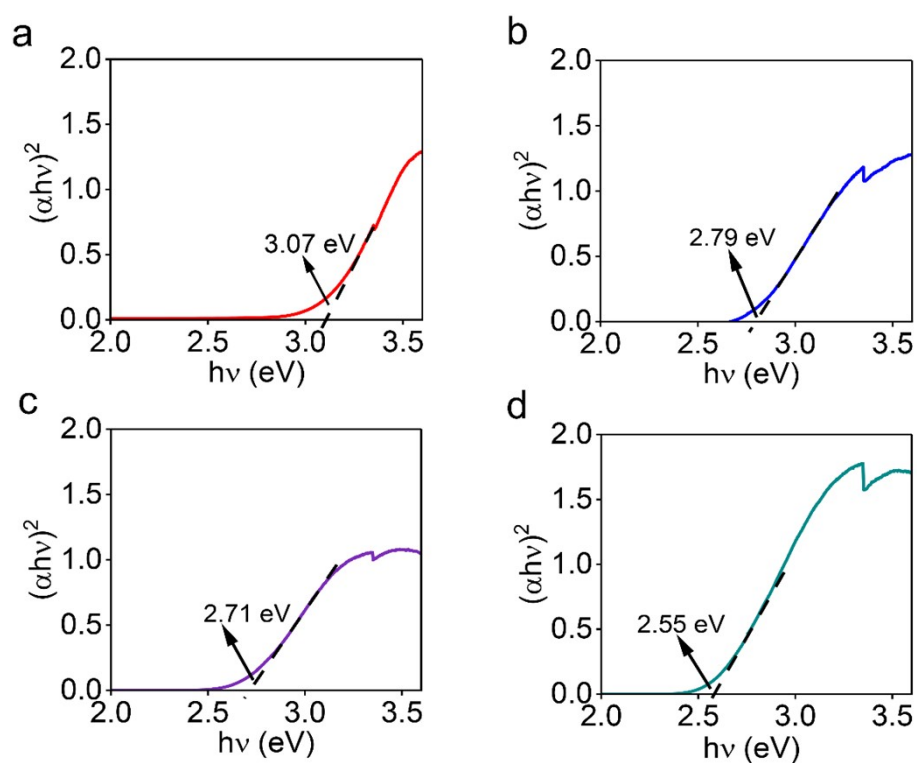


Figure S1. Bandgap calculation results of (a) Zn-In-S colloidal nanocrystals, (b) 1Ag-ZnInS, (c) 2Ag-ZnInS and (d) 3Ag-ZnInS.

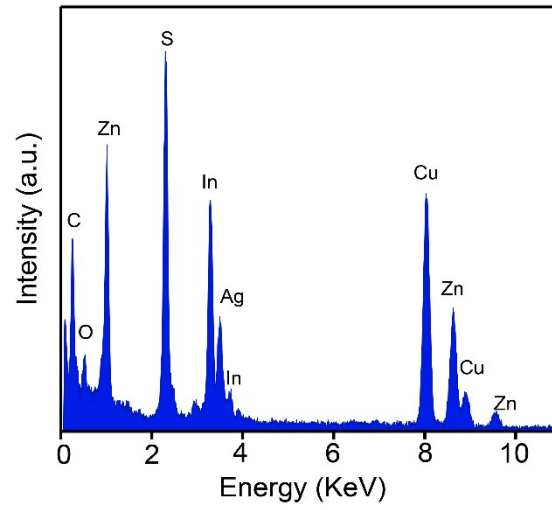


Figure S2. EDX of 2Ag-ZnInS colloidal crystals. The C and Cu elements come from the TEM substrate.

Table S2. Comparison of photocatalytic CO and H<sub>2</sub> evolution rates from CO<sub>2</sub> reduction over different photocatalysts. (Reference:[1-8])

Photocatalysts Cocatalyst: Co(bpy) <sub>3</sub> <sup>2+</sup>	Photocatalysts activity	references
Ag-ZnInS colloidal crystals	CO evolution rate: 30.29 μmol h <sup>-1</sup> H <sub>2</sub> evolution rate: 1.24 μmol h <sup>-1</sup>	This work
TiO <sub>2</sub> nanotubes/ZnIn <sub>2</sub> S <sub>4</sub> heterostructure	CO evolution rate: 17.64 μmol h <sup>-1</sup> H <sub>2</sub> evolution rate: 4.8 μmol h <sup>-1</sup>	Appl. Surf. Sci. 2022, 587, 152895
Ag-In-S QDs	CO evolution rate: 9.2 μmol h <sup>-1</sup> H <sub>2</sub> evolution rate: 3.13 μmol h <sup>-1</sup>	J. Catal. 2021, 401, 271-278
TiO <sub>2</sub> -CoPPcs heterostructures	CO evolution rate: 4.42 μmol h <sup>-1</sup> H <sub>2</sub> evolution rate: 0.76 μmol h <sup>-1</sup>	Mater. Today Chem. 2021, 22, 100589
B <sub>13</sub> P <sub>2</sub>	CO evolution rate: 1.35 μmol h <sup>-1</sup> H <sub>2</sub> evolution rate: 0.3 μmol h <sup>-1</sup>	J. Mater. Chem. A, 2021, 9, 2421-2428
2D TiO-CN	CO evolution rate: 0.85 μmol h <sup>-1</sup> H <sub>2</sub> evolution rate: ~0.08 μmol h <sup>-1</sup>	Nano Res. 2019, 12, 457-462
ZnIn <sub>2</sub> S <sub>4</sub> -In <sub>2</sub> O <sub>3</sub> heterostructures	CO evolution rate: 12.3 μmol h <sup>-1</sup> H <sub>2</sub> evolution rate: ~2.8 μmol h <sup>-1</sup>	J. Am. Chem. Soc. 2018, 140, 5037–5040
In <sub>2</sub> S <sub>3</sub> -CdIn <sub>2</sub> S <sub>4</sub>	CO evolution rate: 3.3 μmol h <sup>-1</sup> H <sub>2</sub> evolution rate: 1.04 μmol h <sup>-1</sup>	J. Am. Chem. Soc. 2017, 139, 1730-1738
Helical g-C <sub>3</sub> N <sub>4</sub>	CO evolution rate: 8.9 μmol h <sup>-1</sup> H <sub>2</sub> evolution rate: 0.3 μmol h <sup>-1</sup>	Angew. Chem. 2014, 126, 12120-12124

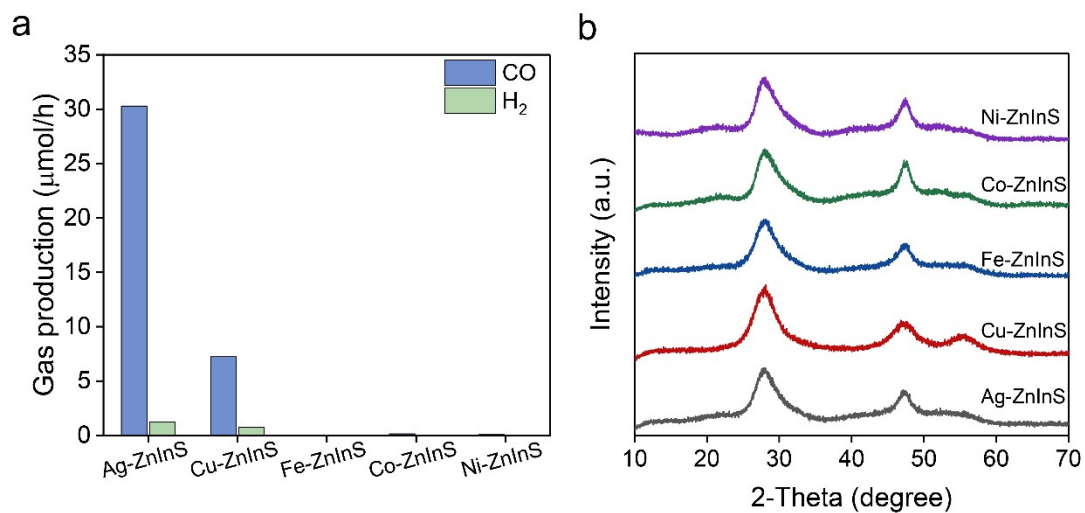


Figure S3. (a) Comparison of photocatalytic CO<sub>2</sub> reduction performances and (b) XRD patterns over different transition metal doped Zn-In-S colloidal nanocrystals.



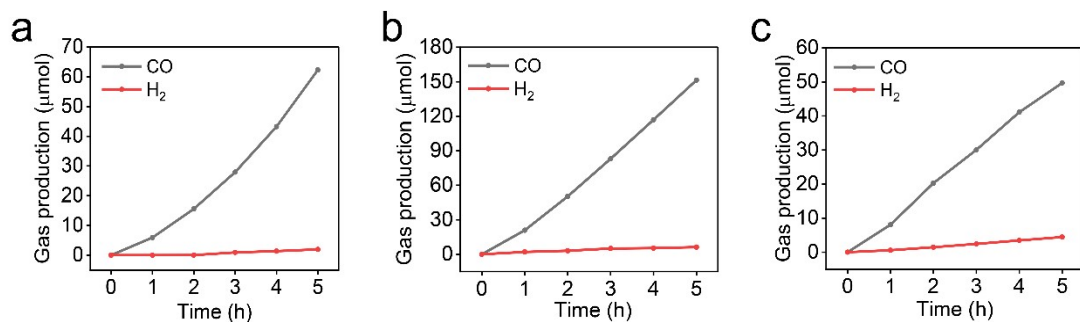


Figure S4. Time-dependent yield of CO and H<sub>2</sub> over (a) 1Ag-ZnInS colloidal nanocrystals, (b) 2Ag-ZnInS colloidal nanocrystals and (c) 3Ag-ZnInS colloidal nanocrystals in the presence of CoBPY as a co-catalyst.

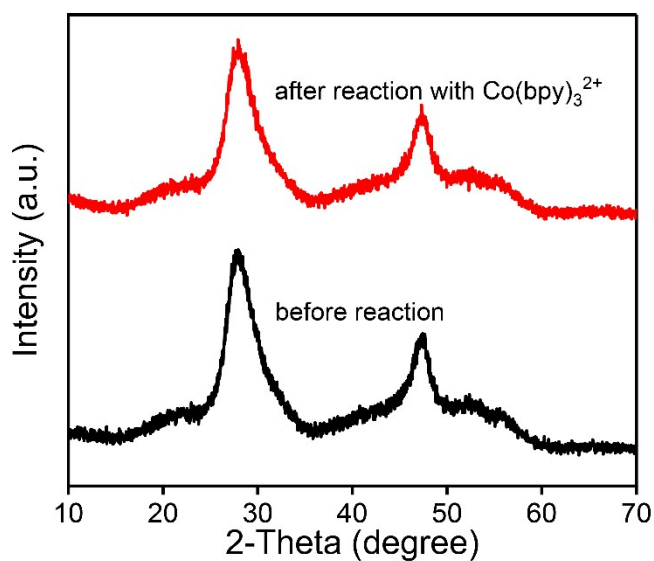


Figure S5. (a) XRD patterns of 2Ag-ZnInS before reaction and after photocatalytic CO<sub>2</sub> reduction reaction in the presence of CoBPY as a co-catalyst.

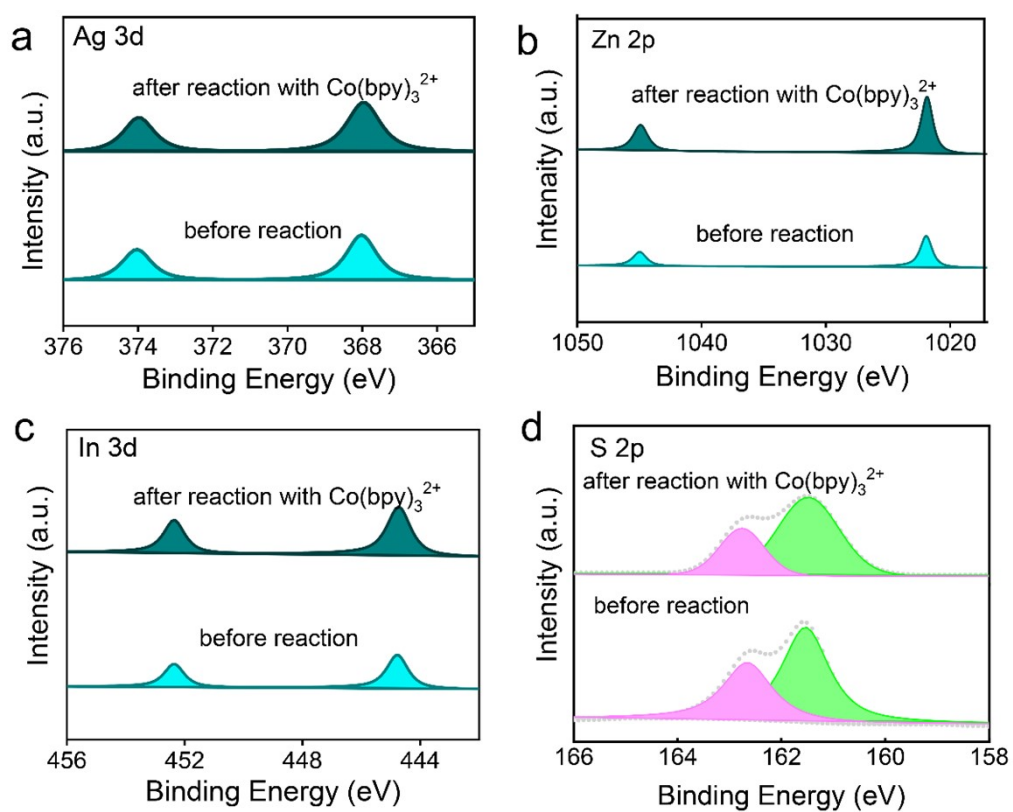


Figure S6. The high-resolution XPS of Ag 3d, Zn 2p, In 3d and S 2p of 2Ag-ZnInS colloidal nanocrystals before and after photocatalytic reaction in the presence of CoBPY as a co-catalyst.

Table S3. Fitting data of time-resolved PL decays over Ag-ZnInS colloidal nanocrystals.

Sample	$\tau_1/\text{ns}$	$A_1$	$\tau_2/\text{ns}$	$A_2$	$\tau_{\text{average}}/\text{ns}$
1Ag-ZnInS	0.9177	528.0739	0.9177	170.6678	0.9177
2Ag-ZnInS	0.8189	634.5900	2.4226	34.1613	1.0392
3Ag-ZnInS	0.9120	734.9465	5.3601	5.7872	1.1088

$\tau_{\text{average}}$  is calculated according to the following equation:

$$\tau_{\text{average}} = \frac{A_1 * \tau_1^2 + A_2 * \tau_2^2}{A_1 * \tau_1 + A_2 * \tau_2}$$

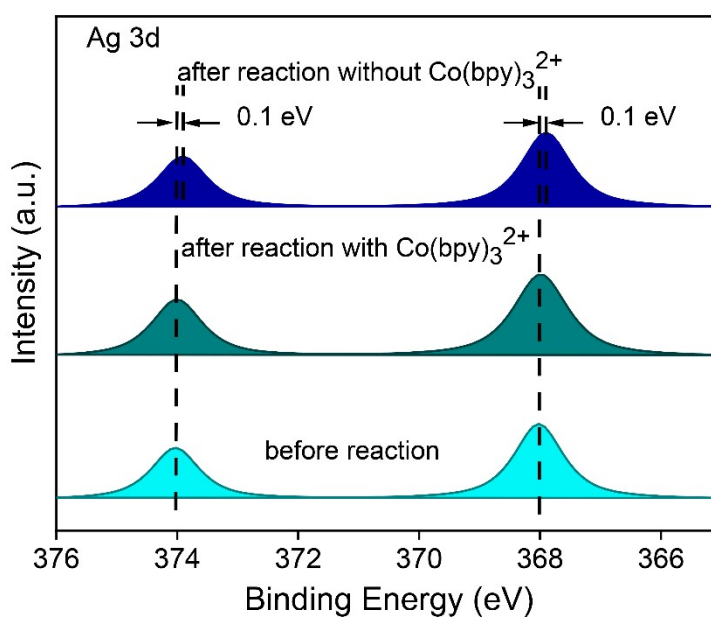


Figure S7. The high-resolution XPS of Ag 3d of 2Ag-ZnInS colloidal nanocrystals before reaction, after photocatalytic  $\text{CO}_2$  reduction reaction in the presence and in the absence of CoBPY as a co-catalyst.

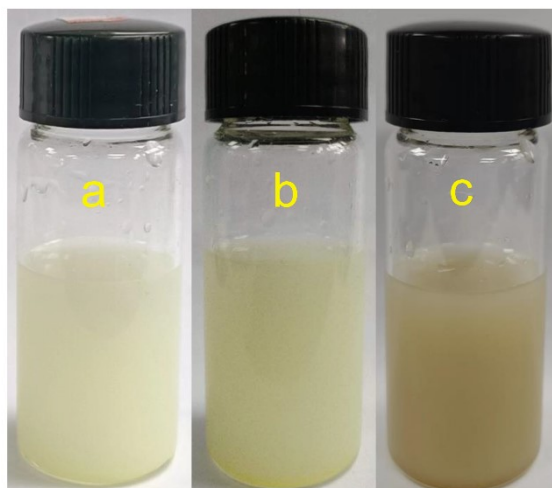


Figure S8. The color change of the reaction solution (a) before reaction , (b) after photocatalytic CO<sub>2</sub> reduction reaction with CoBPY as a co-catalyst and (c) after photocatalytic CO<sub>2</sub> reduction reaction without CoBPY.

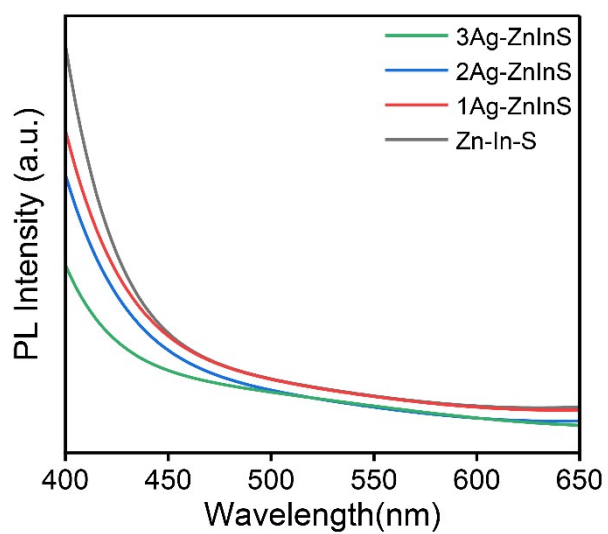


Figure S9. (a) PL spectra of Zn-In-S colloidal nanocrystals and Ag-ZnInS colloidal nanocrystals in the presence of CoBPY.

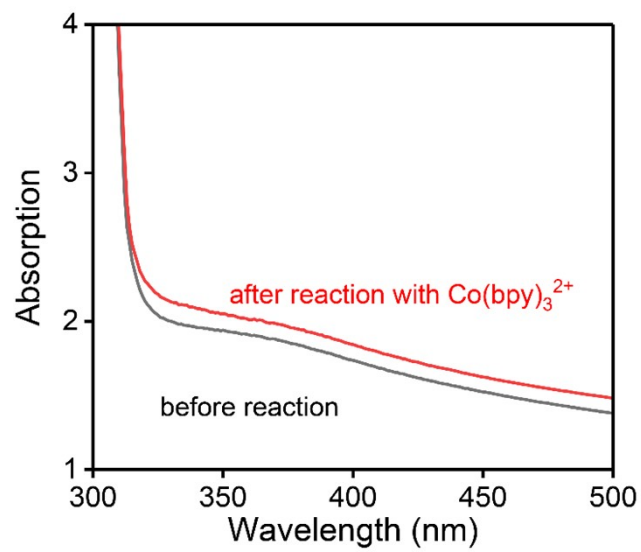


Figure S10. UV-vis absorption spectrum of 2Ag-ZnInS solution before and after photocatalytic CO<sub>2</sub> reduction reaction in the presence of CoBPY as a co-catalyst.

### Supporting Reference:

- [1] E. Kim, K. H. Do, J. Wang, Y. Hong, A. Putta Rangappa, D. Amaranatha Reddy, D. Praveen Kumar and T. K. Kim, *Appl. Surf. Sci.*, 2022, 587, 152895.
- [2] L. Shi, X. Ren, Z. Zhang, Q. Wang, Y. Li and J. Ye, *J. Catal.*, 2021, 401, 271-278.
- [3] K. H. Do, D. Praveen Kumar, A. Putta Rangappa, J. Wang, Y. Hong, E. Kim, D. Amaranatha Reddy and T. Kyu Kim, *Mater. Today Chem.*, 2021, 22, 100589.
- [4] L. Shi, X. Ren, Q. Wang, W. Zhou and J. Ye, *J. Mater. Chem. A*, 2021, 9, 2421-2428.
- [5] S. Tang, X. Yin, G. Wang, X. Lu and T. Lu, *Nano Res.*, 2019, 12, 457-462.
- [6] S. Wang, B. Y. Guan and X. W. D. Lou, *J. Am. Chem. Soc.*, 2018, 140, 5037-5040.
- [7] S. Wang, B. Y. Guan, Y. Lu and X. W. D. Lou, *J. Am. Chem. Soc.*, 2017, 139, 17305-17308.
- [8] Y. Zheng, L. Lin, X. Ye, F. Guo and X. Wang, *Angew. Chem.*, 2014, 126, 12120-12124.